

Antiferromagnetic Order of the Ru and Gd in Superconducting $\text{RuSr}_2\text{GdCu}_2\text{O}_8$

J. W. Lynn¹, B. Keimer², C. Ulrich^{1,2}, C. Bernhard², and J. L. Tallon³

¹*NIST Center for Neutron Research, National Institute of Standards and Technology, Gaithersburg, Maryland 20899 USA*

²*Max-Planck Institute für Festkörperforschung, Heisenbergstrasse 1, D-70569 Stuttgart, Germany*

³*Industrial Research Ltd., P. O. Box 31310, Lower Hutt, New Zealand*

Neutron diffraction has been used to study the magnetic order in $\text{RuSr}_2\text{GdCu}_2\text{O}_8$. The Ru moments order antiferromagnetically at $T_N = 136(2)\text{K}$, coincident with the previously reported onset of ferromagnetism. Neighboring spins are antiparallel in all three directions, with a low T moment of $1.18(6)\mu_B$ along the c axis. Our measurements put an upper limit of $\sim 0.1\mu_B$ to any net zero-field moment, with fields exceeding 0.4T needed to induce a measurable magnetization. The Gd ions order independently at $T_N = 2.50(2)\text{K}$ with the same spin configuration.

74.72.Jt, 75.25.+z, 74.25.Ha, 75.30.Kz

The ruthenate class of materials has been the focus of considerable work recently because of their interesting magnetic and superconducting properties. SrRuO_3 , for example, is a $4d$ band ferromagnet that orders at 165K , [1] while Sr_2RuO_4 is an exotic p -wave superconductor ($T_C = 1.5\text{K}$). [2] Of particular interest here is the recent report of ferromagnetic ordering of the Ru at 133K in $\text{RuSr}_2\text{GdCu}_2\text{O}_8$, while bulk superconductivity is established at lower temperatures as observed in susceptibility and specific heat. [3,4] In these hybrid ruthenate-cuprate systems both the Cu-O and Ru-O planes form very similar square-planar arrays, and the coexistence of superconductivity and long range magnetic order at high temperatures is intriguing. [5] Previous “magnetic-superconductors” such as the Chevrel phases (RMo_6S_8 , R = rare earth ion), [6] borocarbides ($\text{RNi}_2\text{B}_2\text{C}$), [7] and cuprates ($\text{RBa}_2\text{Cu}_3\text{O}_7$ and related materials) [8] show rare earth ordering at low temperature ($\lesssim 10\text{K}$), and almost all are antiferromagnets that do not couple strongly to the superconductivity. The rare occurrence of ferromagnetism, [6] as found in ErRh_4B_4 , HoMo_6S_8 , and HoMo_6Se_8 , revealed the strongly competitive nature of these two cooperative phenomena in the form of long wavelength oscillatory magnetic states at low temperature ($\lesssim 1\text{K}$) and a ferromagnetic lock-in transition that quenches the superconductivity. [9–11] It would then be quite interesting if $\text{RuSr}_2\text{GdCu}_2\text{O}_8$ were a ferromagnetic superconductor with such a high magnetic ordering temperature, as this would suggest [12] a superconducting order parameter of the Fulde-Ferrell-Larkin-Ovchinnikov type [13] that could exhibit π -phase behavior. [14] Our diffraction results, however, demonstrate that the magnetic order of the Ru is predominantly antiferromagnetic, instead making this by far the highest known antiferromagnetic ordering to coexist with superconductivity. An upper limit of $\sim 0.1\mu_B$ is obtained for the ferromagnetic component, consistent with recent magnetization data, and the system is then similar to $\text{ErNi}_2\text{B}_2\text{C}$, where a net magnetization develops below 2.3K . [15] The

Gd moments also order magnetically, but at low temperatures in a manner analogous to previous magnetic-superconductor systems.

A polycrystalline sample of $\text{RuSr}_2\text{GdCu}_2\text{O}_8$ was prepared by the solid state reaction technique, using the ^{160}Gd isotope to avoid the huge nuclear absorption cross section of natural Gd. The single-phase sample weighed $\sim 1.5\text{g}$, has an onset superconducting temperature of 35K and bulk superconducting T_C of 21K , and is the identical sample used in a previous susceptibility and neutron crystallographic study. [16] All the present neutron data were collected at NIST. BT-2 was employed at a neutron wavelength of 2.359\AA , with a pyrolytic graphite filter to suppress higher-order wavelengths. Polarized neutron measurements were carried out with a Heusler monochromator and analyzer. A ^3He refrigerator was employed for the lowest temperature measurements, and a vertical field 7T superconducting magnet for the field measurements. Small angle neutron scattering data were also collected with a wavelength of 5\AA on the NG-1 spectrometer from 6K to 300K . Statistical uncertainties quoted in this article represent one standard deviation.

Fig. 1 shows a portion of the diffraction pattern obtained at a temperature of 16K . The peak at 23.5° is the weak $\{002\}$ nuclear Bragg peak; for comparison, the strong $\{103\}+\{110\}$ Bragg peak at 51.5° has 4809 counts/min. The peaks at 25.8° and 30.8° can be indexed as the $\{\frac{1}{2}, \frac{1}{2}, \frac{1}{2}\}$ and $\{\frac{1}{2}, \frac{1}{2}, \frac{3}{2}\}$ reflections. At a temperature of 150K we see that these peaks have completely disappeared, indicating that they are magnetic and originate from the magnetic ordering of the Ru. There is no change in the nuclear Bragg intensity, where a ferromagnetic component would appear, as clearly indicated by the difference scattering [17] shown at the bottom of the figure. The temperature dependence of the integrated intensity for the $\{\frac{1}{2}, \frac{1}{2}, \frac{1}{2}\}$ peak is shown in Fig. 2. The solid curve is a simple mean field fit to estimate a Néel temperature of $136(2)\text{K}$. This is in excellent agreement with the reported Ru magnetic ordering temperature. [3]

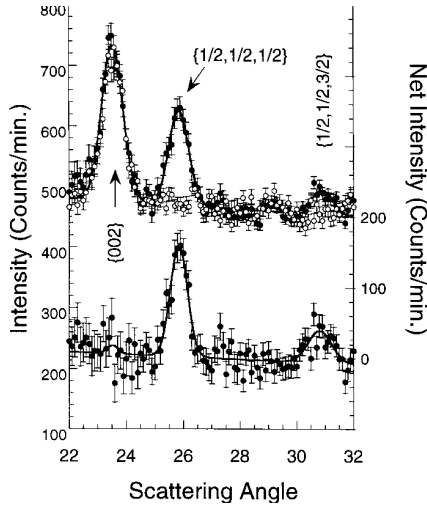


FIG. 1. Portion of a diffraction pattern at 16K, showing the weak nuclear {002} powder peak along with the $\{\frac{1}{2}, \frac{1}{2}, \frac{1}{2}\}$ and $\{\frac{1}{2}, \frac{1}{2}, \frac{3}{2}\}$ Ru antiferromagnetic Bragg peaks. At 150 K the two magnetic peaks have disappeared, while there is no change in the {002} peak, where a ferromagnetic component would be observed. The difference scattering obtained by subtracting the two data sets is shown at the bottom.

The data in Fig. 1 show that the Ru moments order antiferromagnetically, with nearest neighbor spins in all three crystallographic directions aligned antiparallel. The magnetic scattering for a collinear structure is [18]

$$I_M = C |F_M|^2 \frac{m_{hkl} A_{hkl}}{\sin(\theta) \sin(2\theta)} \left\langle 1 - (\hat{\tau} \cdot \hat{M})^2 \right\rangle \quad (1)$$

where C is an instrumental constant, m_{hkl} is the multiplicity of the powder peak with Miller indices hkl for the reciprocal lattice vector τ , A_{hkl} is the absorption factor, \hat{M} is a unit vector in the direction of the moment, and the brackets indicate a powder/domain average. The magnetic structure factor is given by

$$F_M = \sum_{j=1}^N \langle \mu_j^z \rangle f_j(\tau) e^{i\tau \cdot \mathbf{r}_j} e^{-W_j} \quad (2)$$

where $\langle \mu_j^z \rangle$ is the ordered moment and $f_j(hkl)$ is the magnetic form factor for the j^{th} ion at position \mathbf{r}_j in the unit cell, W_j is the Debye-Waller factor, and the sum is over all atoms in the unit cell. The magnetic intensities can be put on an absolute scale by comparison with the nuclear intensities. The intensity for the $\{\frac{1}{2}, \frac{1}{2}, \frac{3}{2}\}$ peak in Fig. 1 is clearly reduced in intensity compared to the $\{\frac{1}{2}, \frac{1}{2}, \frac{1}{2}\}$ peak, and the orientation factor in Eq. (1) then suggests that the direction of the moment is along the tetragonal c axis. The observed intensity ratio of the $\{\frac{1}{2}, \frac{1}{2}, \frac{1}{2}\}$ to $\{\frac{1}{2}, \frac{1}{2}, \frac{3}{2}\}$ peaks is 2.49(40), which is indeed in good agreement with the calculated value of 2.21. Of course, with only two observable magnetic peaks this moment direction assignment is tentative rather than definitive. The ordered Ru moment at low temperatures

is then $1.18(6) \mu_B$, which agrees nicely with the moment of $1.05(5) \mu_B$ obtained from susceptibility, [3]

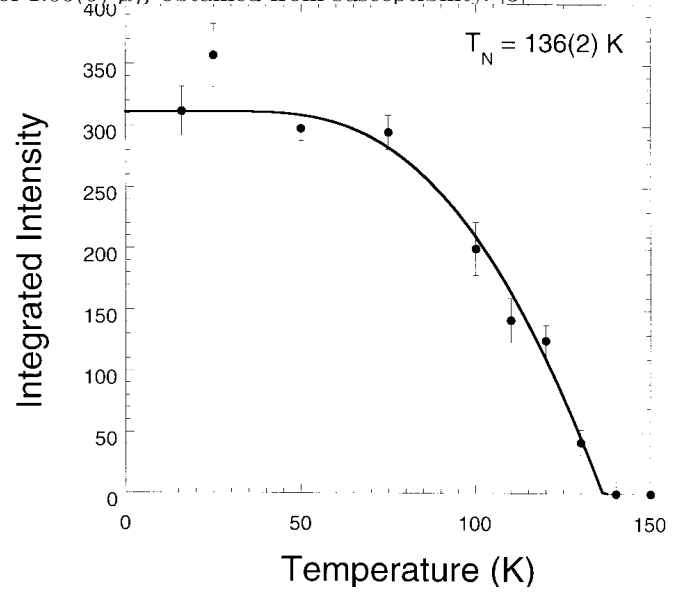


FIG. 2. Integrated intensity of the $\{\frac{1}{2}, \frac{1}{2}, \frac{1}{2}\}$ Ru magnetic Bragg peak vs. T . The curve is a fit to mean-field theory.

Any ferromagnetic contribution to the scattering will occur at the same positions as the nuclear Bragg peaks, and the data in Fig. 1 indicate no magnetic contribution to the {002} peak within experimental error. We measured the intensities of the ten lowest-angle nuclear Bragg reflections above and below the Ru magnetic ordering temperature, and these data provide an upper limit of $\sim 0.1 \mu_B$ to any ferromagnetic component. This result was substantiated by polarized beam measurements, although the error limit was comparable to that obtained with unpolarized neutrons. We also monitored the flipping ratio of the intensity transmitted through the sample to determine if there were any depolarization of the beam as might be expected for a ferromagnet. No change with temperature was observed. Finally, we measured the small angle scattering on NG-1 in an attempt to see any critical scattering associated with ferromagnetic correlations that might develop, but no scattering was observed. Therefore the neutron data so far do not reveal the ferromagnetic component associated with the Ru ordering.

The field dependence of the magnetic scattering of the $\{\frac{1}{2}, \frac{1}{2}, \frac{1}{2}\}$ and {002} peaks, corresponding to the antiferromagnetic order and induced ferromagnetic moment, respectively, is shown in Fig. 3. A temperature of 80 K was chosen for these measurements since this is well below the Ru ordering temperature so that the sublattice magnetization is near its saturated value, but it is high enough in temperature that the Gd paramagnetic moment should not dominate the net magnetization except at the highest fields. No significant change in either intensity is observed up to $\sim 0.4T$. With further increase

of field the intensity of the antiferromagnetic reflection begins to decrease, while the induced magnetization increases. At the highest field of $7T$ there is no significant antiferromagnetic intensity remaining (as indicated by full angular scans), while the induced magnetization corresponds to a net moment of $1.4(1) \mu_B$ perpendicular to c . The calculated induced Gd paramagnetic moment is shown by the dashed curve, and for fields above $\sim 0.4T$ the data systematically lie above the curve indicating a Ru contribution. However, the value is $\sim 0.2 \mu_B$, which suggests the Ru moments are rotating into another antiferromagnetic (spin-flop) structure, rather than becoming fully aligned with the field. Returning to zero field, all the peaks recover their zero-field intensities, indicating that the effect of the field is reversible, and also that no preferred orientation of the loose powder particles occurred when the field was applied. The Gd anisotropy is very small since it is an S-state ion. The low spin-flop field and the lack of any field-induced preferred orientation then suggests that the Ru crystalline anisotropy is also relatively weak, indicating that a Heisenberg Hamiltonian is appropriate to describe the Ru spin system.

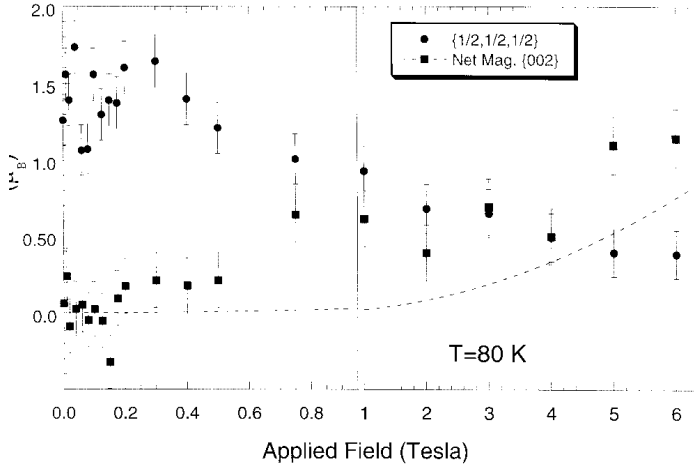


FIG. 3. Field dependence of the square of the antiferromagnetic moment and induced ferromagnetic moment (\propto normalized observed intensity) at 80 K. An expanded scale has been used at low fields for clarity. The dashed curve represents the induced Gd moment.

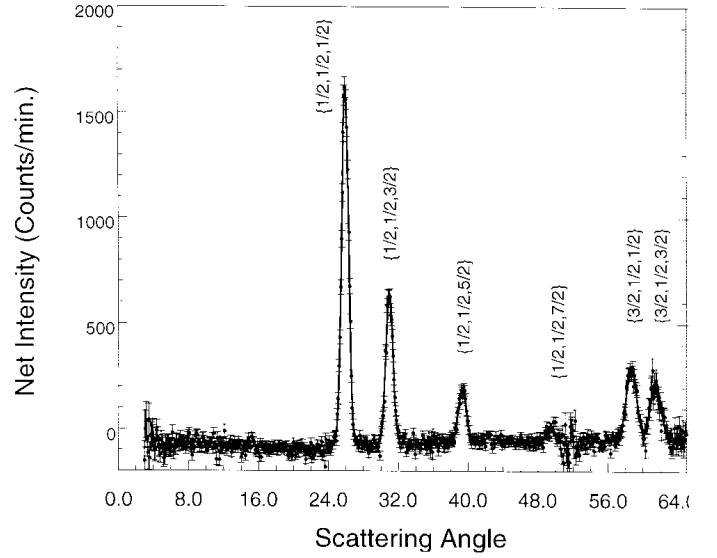


FIG. 4. Magnetic diffraction pattern for Gd, obtained by subtracting the data at 1.6 K from the data at 5 K.

We now turn to measurements of the Gd magnetic order. Fig. 4 shows the magnetic diffraction pattern, obtained by subtracting the data at 5 K from the data at 1.6 K, below T_N . [17] We see that the peak positions and relative intensities are identical to that for the Ru, so that nearest-neighbor Gd spins are also coupled antiferromagnetically along all three crystallographic directions, with the moment direction along the tetragonal c axis. The calculated and observed intensities then agree to within the statistical uncertainties.

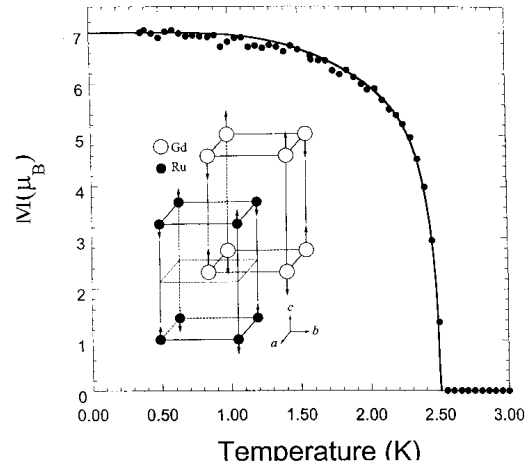


FIG. 5. Gd sublattice magnetization vs. T . The Néel temperature is 2.50 K. The inset shows the magnetic structures for the Ru and Gd.

The temperature dependence of the sublattice magnetization for the Gd is shown in Fig. 5. We obtain the

expected $7 \mu_B$ moment within experimental uncertainties at low T. Near T_N a small correction has been applied to the observed intensity to account for critical scattering, and the solid curve is a fit to a modified power law, with a fitted ordering temperature of 2.50(2) K. The sharpness of the ordering might at first be surprising since the Ru and Gd magnetic structures are identical, and hence one might expect them to be strongly coupled, smearing the Gd order parameter. However, the Gd ions sit at the body-centered position of the simple tetragonal Ru lattice. The antiferromagnetic magnetic structure for the Ru then results in a cancellation of the average interaction between the Gd and Ru (Fig. 4), rendering the two spin systems fully frustrated (neglecting quantum fluctuations) with respect to each other and thus behaving independently to a good approximation. It is noteworthy that this frustration is relieved by a (zero-field) ferromagnetic component on the Ru sublattice, so that the sharpness of the Gd order parameter is another indication that the Ru magnetic structure can have only a modest net moment.

The Ru antiferromagnetic moment we observe is in good agreement with the moment obtained from susceptibility, accounting for essentially the full ordered moment. Our experimental upper limit of $\sim 0.1 \mu_B$ on the ferromagnetic component is consistent with the spontaneous moment derived from low-field data, but is inconsistent with band structure calculations predicting full ferromagnetic spin polarization of the Ru subsystem. [12] The crystallographic data [16,4] indicate a rotation of the RuO_6 octahedra about the c -axis, with a small rotation around an axis perpendicular to c . It is the latter rotation that would be needed for conventional mechanisms such as antisymmetric exchange or single-ion anisotropy to produce a canting and net Ru moment as observed in a variety of measurements. [3,4] In any case, the antiferromagnetism is dominant, and the coexistence of superconductivity with the high ordering temperature and consequent large exchange interactions of the Ru make this an especially interesting system for further investigations.

Acknowledgments. We would like to thank R.W. Erwin and Q. Huang for their assistance, and J. D. Jorgensen for communicating their results prior to publication.

-
- [1] J. M. Longo, P. M. Raccah, and J. B. Goodenough, *J. Appl. Phys.* **39**, 1327 (1968).
 - [2] K. Ishida, H. Mukuda, Y. Kitaoka, K. Asayama, Z. O. Mao, Y. Mori, and Y. Maeno, *Nature (London)* **396**, 658 (1998).
 - [3] C. Bernhard, J. L. Tallon, Ch. Niedermayer, Th. Blasius, A. Golnik, E. Brücher, R. K. Kremer, D. R. Noakes, C. E. Stronach, and E. J. Ansaldo, *Phys. Rev. B* **59**, 14099 (1999). A. Fainstein, E. Winkler, A. Butera, and J. Tallon, *ibid* **B60**, R12597 (1999); J. L. Tallon, C. Bernhard, M. Bowden, P. Gilberd, T. Stoto and D. Pringle, *IEEE Trans. Appl. Supercon.* **9**, 1696 (1999); C. Bernhard, J. L. Tallon, E. Brücher and R. K. Kremer (preprint).
 - [4] A. C. McLaughlin, W. Zhou, J. P. Attfield, A. N. Fitch, and J. L. Tallon, *Phys. Rev. B* **60**, 7512 (1999).
 - [5] I. Felner, U. Asaf, Y. Levi, and O. Millo, *Phys. Rev. B* **55**, R3374 (1997).
 - [6] For a review see *Topics in Current Physics*, edited by Ø. Fischer and M. B. Maple (Springer-Verlag, New York, 1983), Vols. 32 and 34.
 - [7] J. W. Lynn, S. Skanthakumar, Q. Huang, S. K. Sinha, Z. Hossain, L. C. Gupta, R. Nagarajan, and C. Godart, *Phys. Rev. B* **55**, 6584 (1997).
 - [8] For a recent review see J. W. Lynn and S. Skanthakumar, *Handbook on the Physics and Chemistry of Rare Earths*, Ed. by K. A. Gschneidner, Jr., L. Eyring, and M. B. Maple (in press).
 - [9] D. E. Moncton, D. B. McWhan, P. H. Schmidt, G. Shirane, W. Thomlinson, M. B. Maple, H. B. MacKay, L. D. Woolf, Z. Fisk, and D. C. Johnston, *Phys. Rev. Lett.* **45**, 2060 (1980); S. K. Sinha, G. W. Crabtree, D. G. Hinks, and H. A. Mook, *Phys. Rev. Lett.* **48**, 950 (1982).
 - [10] J. W. Lynn, G. Shirane, W. Thomlinson, and R. N. Shelton, *Phys. Rev. Lett.* **46**, 368 (1981).
 - [11] J. W. Lynn, J. A. Gotaas, R. W. Erwin, R. A. Ferrell, J. K. Bhattacharjee, R. N. Shelton, and P. Klavins, *Phys. Rev. Lett.* **52**, 133 (1984).
 - [12] W. E. Pickett, R. Weht, and A. B. Shick, *Phys. Rev. Lett.* **83**, 3713 (1999).
 - [13] P. Fulde and R. A. Ferrell, *Phys. Rev.* **135**, A550 (1964); A. I. Larkin and Yu. N. Ovchinnikov, *Sov. Phys. JETP* **20**, 762 (1965).
 - [14] V. Prokic, A. I. Buzdin, and L. Dobrosavljevic-Grujic, *Phys. Rev. B* **59**, 587 (1999).
 - [15] P. C. Canfield, S. L. Bud'ko, and B. K. Cho, *Physica C* **262**, 249 (1996).
 - [16] O. Chmaisam, J. D. Jorgensen, H. Shaked, P. Dollar, and J. L. Tallon (preprint).
 - [17] Addition details are given in H. Zhang, J. W. Lynn, W-H. Li, T. W. Clinton and D. E. Morris, *Phys. Rev. B* **41**, 11229 (1990).
 - [18] G. E. Bacon, *Neutron Diffraction*, (Clarendon, Oxford, 1975).
-
- [1] J. M. Longo, P. M. Raccah, and J. B. Goodenough, *J. Appl. Phys.* **39**, 1327 (1968).
 - [2] K. Ishida, H. Mukuda, Y. Kitaoka, K. Asayama, Z. O. Mao, Y. Mori, and Y. Maeno, *Nature (London)* **396**, 658 (1998).
 - [3] C. Bernhard, J. L. Tallon, Ch. Niedermayer, Th. Blasius,